Spectroscopic Characterization of Mineralogy Across Vesta: Evidence of Different Lithologies

M.C. De Sanctis[1*], E. Ammannito[1], G. Filacchione[1], M.T. Capria[1], F. Tosi[1], F.Capaccioni[1], F. Zambon[1], F. Carraro[1], S.Fonte[1], A. Frigeri[1], R. Jaumann[2], G. Magni[1], S. Marchi[3], T.B. McCord[4], L.A. McFadden[5], H.Y. McSween[6], D.W. Mittlefehldt[7], A. Natheus[8], E. Palomba[1], C.M. Pieters[9], C.A. Raymond[10], C.T. Russell[11], D. Turrini[1]

[1] Istituto Nazionale di Astrofisica, Rome, Italy; [2] Institute of Planetary Research, DLR, Berlin, Germany; [3]NASA Lunar Science Institute, Boulder, USA; [4]Bear Fight Institute, Winthrop, USA; [6]Department of Earth and Planetary Sciences, University of Tennessee, Knoxville, TN 37996, USA; [8] Max Planck Institut fur Sonnensystemforschung, Katlenburg-Lindau, Germany; [10]Jet Propulsion Laboratory, California Institute of Technology, Pasadena, CA;[11] Institute of Geophysics and Planetary Physics, University of California, Los Angeles, CA 90095-1567, USA.

*To whom correspondence should be addressed. E-mail: mariacristinadesanctis@iasf-roma.inaf.it

The average spectrum of Vesta, obtained by VIR in the range 0.25-5.1 μm, shows clear evidence of absorption bands due to pyroxenes and thermal emissions beyond 3.5 μm. Vesta shows considerable variability across its surface in terms of spectral reflectance and emission, band depths, bands widths and bands centers, reflecting a complex geological history. Vesta's average spectrum and inferred mineralogy resemble those of howardite meteorites. On a regional scale, significant deviations are seen: the south polar 500km Rheasilvia impact crater has a higher diogenitic component, and equatorial regions show a higher eucritic component. This lithologic distribution, with a concentration of Mg-pyroxenes in the Rheasilvia area, reinforces the hypothesis of a deeper diogenitic crust excavated by the impact that formed the Rheasilvia crater, and an upper eucritic crust, whose remnants are seen in the equatorial region. This scenario has implications for Vesta differentiation, consistent with magma ocean models. However, serial magmatism models could also have concentrated pyroxene cumulates in plutons emplaced within the lower crust.

Asteroid 4 Vesta was identified as having a surface of basaltic material through visible/near-infrared reflectance spectroscopy utilizing ground-based telescopes (1). Vesta's spectrum was shown to have strong absorption features centered near 0.9 and 1.9 μm, indicative of pyroxenes, and was shown to be similar to the spectra of HED (howardite, eucrite and diogenite) meteorites (2). This led to the hypothesis that Vesta was the parent body of the HED clan (3,4). The hypothesis gained widespread support when it was shown that numerous, basaltic asteroids are distributed in space from near Vesta out to the 3:1 Kirkwood gap and the *v6* resonance, and which were able, by means of gravitational perturbations and collisions, to send meteoroids into Earth-crossing orbits (5). Since then, geochemical, petrologic, and geochronologic studies of

HEDs have allowed the development of models for the magmatic evolution of Vesta. The consensus view is that the HEDs parent asteroid was substantially melted early in its history through heating by decay of ^{26}Al and ^{60}Fe, forming a molten core topped by a shell of molten silicates. Cooling and crystallization of the silicate global magma ocean produced an olivine-dominated mantle, a lower crust rich in low-Ca pyroxene (diogenites), and an upper crust of basaltic flows and gabbroic intrusions (eucrites) (6-8). However, some HEDs are inconsistentwith this scenario, and some workers favor a model with less melting and serial magmatism (9-11). The Visual-Infrared Mapping Spectrometer VIR (12) on the Dawn spacecraft allows us to verify the paradigm that the HED meteorites are samples from Vesta and evaluate competing hypotheses about its differentiation (13).

VIR is a high-resolution imaging spectrometer with a spectral range of 0.25-5.01 μm and a spatial sampling of 250 μrad (12). It combines two data channels in one compact instrument: the visible channel covers the spectral range, 0.25-1.07 μm, and the infrared channel, the 0.95-5.1 μm range, with a spectral sampling of $\Delta\lambda_{VIS}$ = 1.8 nm/band and $\Delta\lambda_{IR}$ = 9.8 nm/band, respectively.

VIR obtained spatially resolved hyperspectral images of Vesta, during the approach and survey phases (see SOM) with a spatial sampling varying from 1.3 to ~0.7 km. The orientation of the Vesta spin axis and the Dawn orbital characteristics allowed more than 65% of the surface to be imaged, ranging from the south pole up to about 40 degrees north latitude. VIR acquired about four million spectra of Vesta's surface under different illumination conditions, with phase angles ranging from 67.8° to a minimum value of 7.9°.

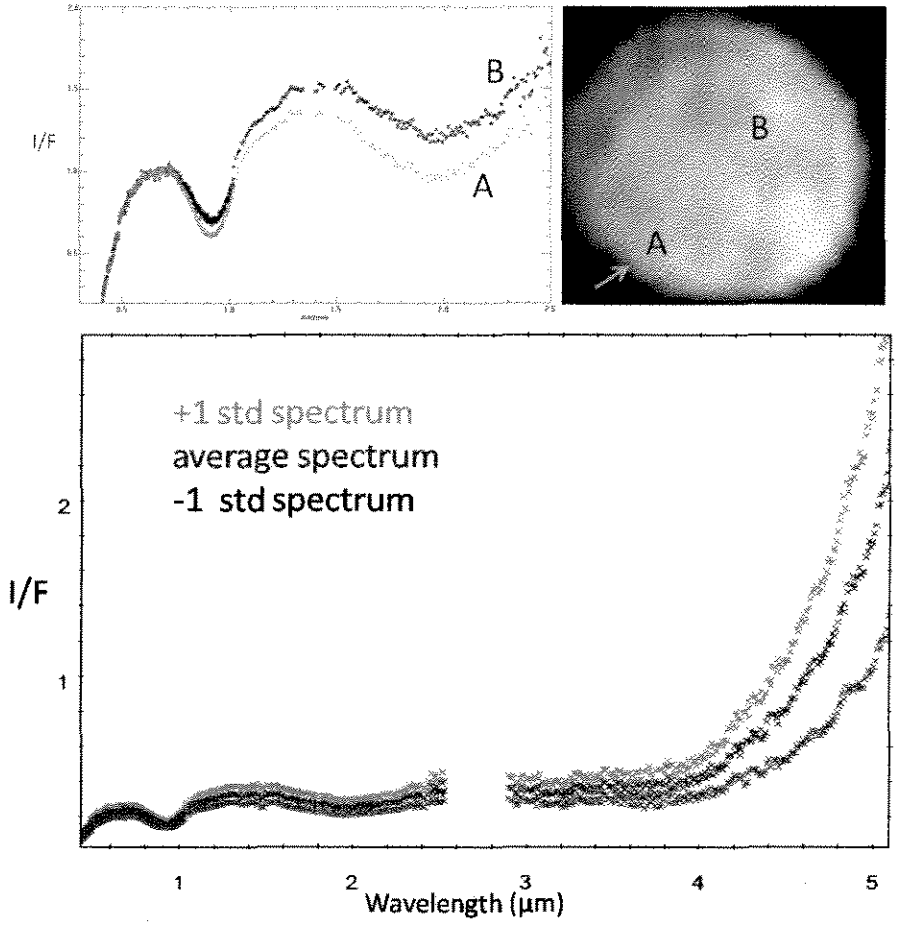

Figure 1. Top panel: left - Spectra of regions A and B as indicated in the VIR Vesta image on the right; the spectra have been normalized at 0.7 μm in order to highlight differences in band depth and shape. Right - Image obtained by assigning red, green and blue to 0.92, 0.62 and 0.44 μm bands, respectively (spatial resolution of about 25 km The south pole is indicated by the arrow. Bottom: average Vesta spectrum with ± 1 standard deviation of the average shown. The data between 2.5 and 2.8 μm have been removed because the data are not yet fully calibrated in this region; the "feature" at 1.4 μm is an artifact.

The first data, at a resolution twice that of the Hubble Space Telescope (HST), were obtained during the Approach phase on 30 June 2011 (**Fig. 1**) from a distance of about 99,200 km. The acquired spectra show clear evidence of pyroxenes absorption bands at 0.9 and 1.9 μm (hereafter labeled as BI and BII). The spectra show considerable variability, with different regions of Vesta being characterized by distinctly different band depths, band widths, band shapes of the pyroxene bands (**Fig. 1, top left**). Beyond ~3.5 μm, the surface thermal emission becomes increasingly important, and the spectral variations also reflect the local time changes, from sunset to sunrise, with the corresponding surface temperature changes (17) (**Fig. 1, bottom**).

The color composite image of Vesta (**Fig. 1, top right**) demonstrates that there are large-scale variations in the spectral properties of the surface material, more so than on other asteroids imaged by spacecraft and Mercury (14-16). In this image, the reddish color of the northern hemisphere indicates greater reflectivity at 0.92 μm, and hence shallower pyroxene absorption bands compared to the southern hemisphere. This is shown in the representative spectra from

regions A and B. Region A in the southern hemisphere shows stronger absorption at 0.92 μm relative to the continuum at 0.7 μm than does region B (**Fig. 1, top left**).

The large-scale spectral diversity, on the order of hundreds of kilometers, is confirmed by the data acquired during the survey orbit (see SOM) where the nominal spatial sampling was about ~700 m. VIR observed mostly the southern hemisphere, dominated by the south polar impact basin, Rheasilvia, and covered latitudes as large as almost 45° north (the northern polar region was in permanent shadow during Survey orbits). Although the surface of Vesta shows spectral variations at both large and small scales, the materials on the surface are always dominated by basaltic materials, as indicated by the ubiquitous BI and BII pyroxene signatures. These bands are caused by absorption of photons, primarily by Fe^{2+} and Mg in the pyroxene M1 and M2 site (18).

A global-scale spectral dichotomy is evident between the equatorial and southern regions as shown on maps of BI and BII depths and BII centers (**Fig. 2**). The two pyroxene bands show distinct characteristics between the two regions. In the region at the south pole, the bands are, on average, deeper and wider (larger band areas) than in the equatorial region. In general, BI depths in the equatorial region are ~0.35-0.4, while those in the Rheasilvia basin commonly are 0.45-0.55. Similarly, BII depths in the equatorial region typically have values of ~0.2-0.15, while in the southern region the values are of the order of 0.3-0.25. The depth of an absorption band is mainly determined by the abundance of the absorber and by the grain size distribution of the soil. Thus, the VIR data indicate that the region of the Rheasilvia basin is richer in pyroxene than the equatorial regions of Vesta or that the regolith in this region has a larger grain size distribution. The latter would be consistent with a less collisional grinding in the southern region, associated with the younger age of the Rheasilvia basin (19, 20, 21).

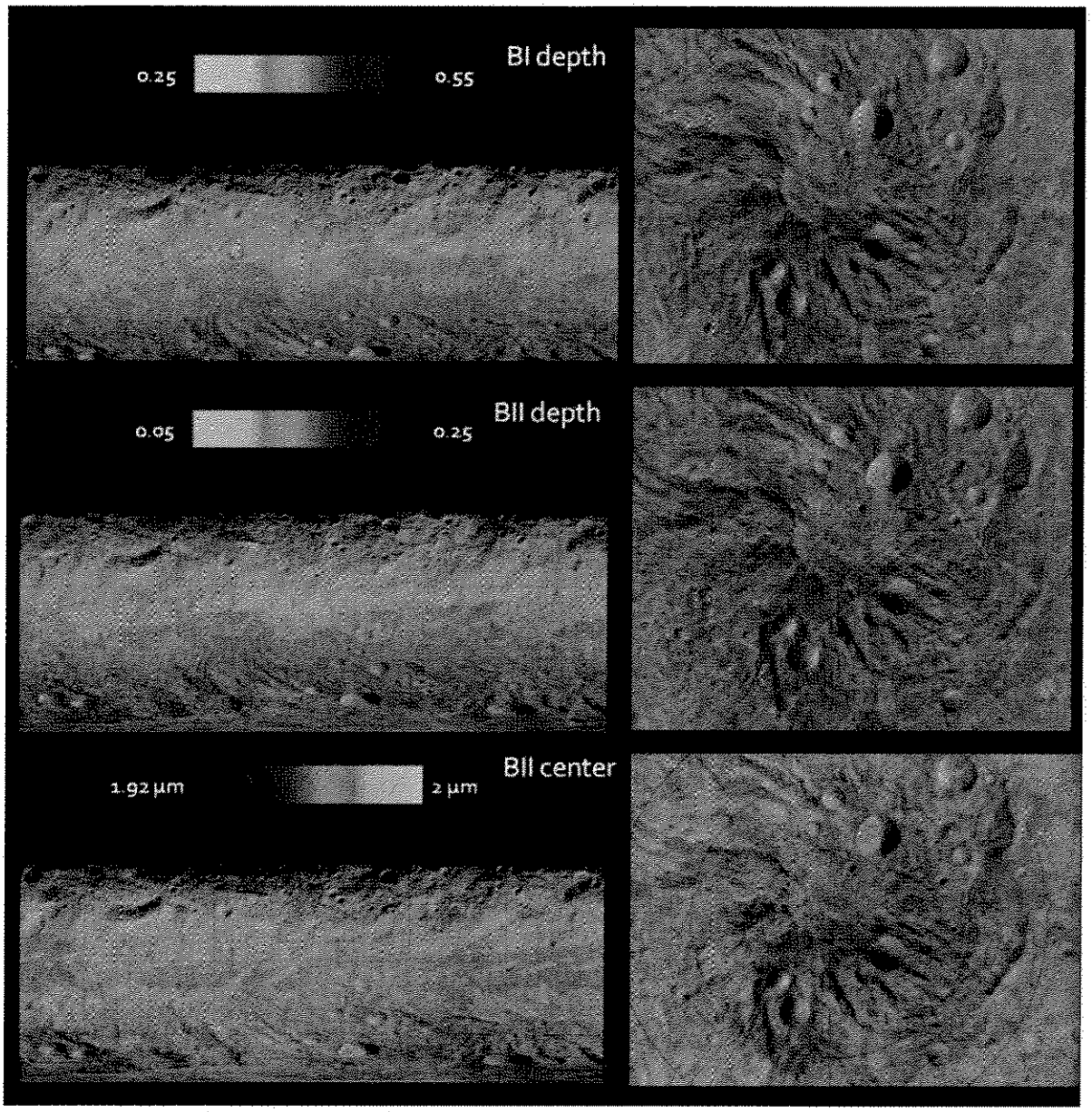

Figure 2. The panels represent cylindrical projections of spectral parameters obtained by VIR: a) BI depths; b) BII depths; c) BII centers. Band depths are defined as in (22). Band centers are computed after continuum removal (see SOM).

The global dichotomy evident in the distributions of pyroxene band depths is also show by variations in band center wavelengths (**Fig. 2c**). Laboratory studies have shown that band centers for the 0.9 and 1.9 µm pyroxene absorption features are systematically different for diogenites and eucrites (23). To directly compare Vesta band centers with HEDs, we computed the band centers of HEDs by applying the same method to both the datasets. As expected, BI and BII centers are at slightly shorter wavelengths for diogenites (BI <0.926µm and BII <1.95 µm) than for eucrites (BI >0.927 µm and BII >1.96 µm), a consequence of the more magnesian pyroxenes with lower Ca concentrations in the former (e.g. 22). Howardites, due to their mixed nature, lie in between, but partially overlap the fields of diogenites and eucrites.

Maps of the BII centers show that they are at generally longer wavelengths in the equatorial regions than in the southern polar region, and that the global variation in BII centers often corresponds closely to, but inversely with, band depth variations (**Fig. 2**). Equatorial regions are prevalently characterized by BII centers at longer wavelengths (**Fig. 2c**) corresponding also to intermediate/shallow band depths (**Fig. 2a,b**). In contrast, in the Rheasilvia basin, the BII centers are at shorter wavelengths (**Fig. 2c**) and these often correspond to the deepest pyroxene absorption bands (**Fig. 2a,b**).

The general correlation between band depths and band centers can be interpreted in terms of diogenite/eucrite content of the different terrains. Diogenites contain ~90-95 vol% pyroxene (23) while basaltic eucrites contain ~50 vol% pyroxene (24), implying that, for a given grain size, the diogenites spectra have stronger bands with respect to eucrites. The correspondence of stronger pyroxene absorption with lower BII (and BI) centers in the Rheasilvia basin indicate a more diogenite-rich lithology dominating the materials exposed on the surface in this region. The Rheasilvia basin is the largest impact structure on Vesta, and it excavated deep into the crust (19, 21). The spectral data indicate that this lower crustal material is mineralogically different, being more diogenite-rich. The spectra of equatorial regions have band centers shifted to longer wavelengths, indicating more Fe-rich pyroxenes (**Fig. 2c**), and intermediate/shallow band depths, indicating primarily lower pyroxene abundance. This correlation demonstrates that there is a greater eucrite component in the surface materials of the equatorial regions. Furthermore, the equatorial region is not uniform. In particular, an extensive area at about 40° east longitude has measurably deeper absorption bands and shorter wavelengths, demonstrating a lower proportion of eucritic material on that area of the surface. The mineralogy of the equatorial region is likely affected also by Rheasilvia ejecta (19, 21) and these VIR measurements generally support the Vesta paradigm that the lower crust is dominated by pyroxene-rich material.

VIR data show that Vesta's surface not only has large-scale variations, but also different characteristics at local scale, i.e. bright and dark localized areas (see SOM). Geologic processes have altered the Vestan crust since its formation (19-21). In fact, Vesta's geological structures at scales of tens of kilometers often show associated spectral differences. Most of the structures are impact craters showing copious ejecta and mass movements. Differences in surface materials composition, abundances or physical properties, can be enhanced by using different spectral band combinations to obtain false colour images. **Fig. 3** shows an example from the Oppia region. In the visible portion of the spectrum, the terrain shows variations in albedo and red slope indicating differences in surface materials (**Fig. 3, left**). The central panel in **Fig. 3** is constructed from two visible bands (B=0.55 μm, G=0.75 μm) and an IR band (R=0.93 μm) approximately centered on pyroxene BI. The area around the fresh crater (E) and the crater floor (F) are characterized by shallower BI, indicating material poor in pyroxene relative to the surrounding terrain. The cratering process results in inverted stratigraphy of roughly the upper third of the target lithology in the ejecta blanket nearest the rim (e.g. 25). The crater floor and material partway up the walls have a reddish hue similar to the ejecta just outside the rim, consistent with the lower layers in this crater being composed of rock poorer in pyroxene. The cyan color in **Fig. 3** (center) indicates that the soils just below the rim (H) have stronger absorption in pyroxene BI, and thus have higher pyroxene content. However, band depth variations can be associated also to grain size differences. VIR reveals that the impact generating the Oppia crater exposed different kinds of materials, suggesting a complex stratigraphy on Vesta. The right panel in **Fig. 3**

highlights the BI absorption feature. The small crater (S) near the rim of the large Oppia crater is now clearly seen, surrounded by a halo of bright and green materials, similar to the layer exposed in Oppia upper walls, suggesting a similar composition.

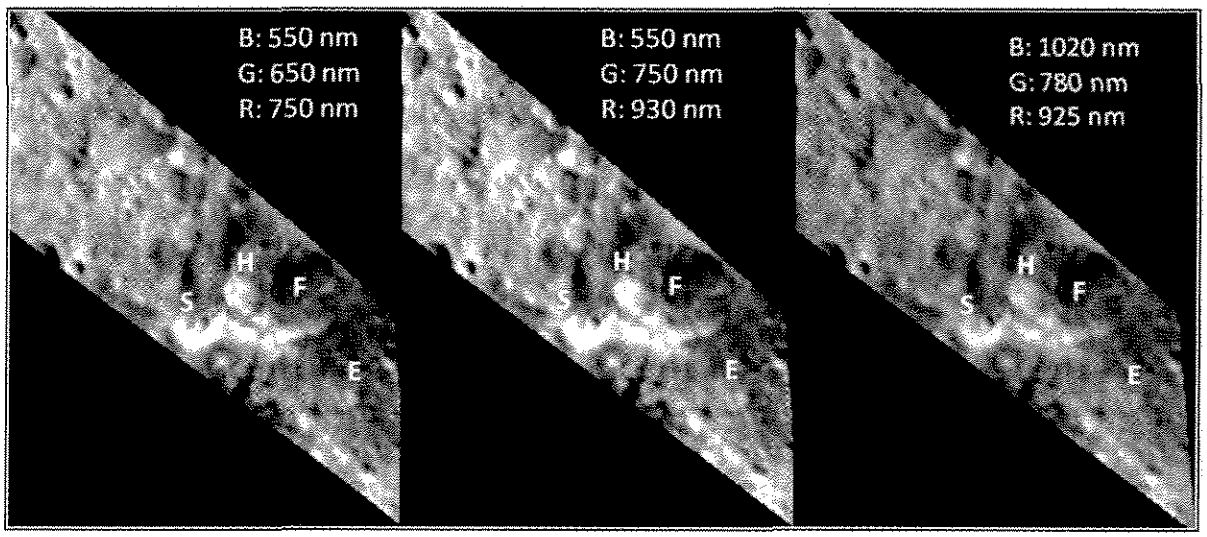

Figure 3. Portion of Vesta surface in the Oppia region. Left: an image made by combining bands in the visual continuum shows terrains differing mainly due to the brightness. Center: this image, made using two bands in the visual continuum (B:550 nm, G:750 nm) and the pyroxene absorption band (R:930 nm), shows lithologic diversity around the central crater with copious "red" ejecta corresponding to shallower pyroxene absorption band depths. The crater walls are characterized by "cyan" materials corresponding to deeper pyroxene absorption bands). Furthermore, a distinction between reddish material around the crater and the brown-green terrain on its left is clearly seen. Right: an image made by combining colors defining the 930 micron band depth, where the small carter near the Oppia rim (S) is clearly seen.

Pyroxenes are the most prominent spectral features on Vesta on the few-hundred-meters scale, and on average, the Vesta spectral parameters resemble those of howardites (see SOM). The VIR spectra are thus consistent with a surface covered by howardite-like materials containing varying proportions of eucrite or diogenite at different locations across the surface. This firmly confirms the link between Vesta and the HED clan of meteorites, increasing our confidence in using laboratory studies of those meteorites to further understand the formation and evolution of Vesta.

Vesta shows large color and spectral variation, much more than for any other asteroid, Mercury or the Moon. Spectral variations often reflect geological structures, indicating a complex geological and evolutionary history for Vesta, a history more similar to that of the terrestrial planets than to other asteroids. The occurrence of diogenite at depth is consistent with magma ocean models for Vesta's differentiation, which could have produced a lower crust or upper mantle containing significant cumulus pyroxene. However, serial magmatism models could also have concentrated pyroxene cumulates in plutons emplaced within the lower crust. In the latter case, the plutons should also contain rocks of complementary composition, such as cumulate

eucrites (gabbros). VIR data constrain the mineralogy of Vesta, providing new insights into the processes that produced the solar system's smallest planet.

References:

1. T. B. McCord, J. B. Adams,T. V. Johnson, *Science* **168,** 1445-1447 (1970).
2. Feierberg and Drake, *Science* **209**, 805-807 (1980).
3. G. J. Consolmagno, M. J. Drake, *Geochim. Cosmochim. Acta* **41,** 1271-1282 (1977).
4. M. J. Drake, In *Asteroids*, T. Gehrels, Ed. (Univ. Arizona Press, Tucson, AZ) 765-782 (1979).
5. R. P. Binzel *et al.*, *Icarus* **128,** 95-103 (1997).
6. K. Righter, M. J. Drake, *Meteor. Planet. Sci.* **32,** 929-944 (1997).
7. P. H. Warren, *Meteor. Planet. Sci. 32,* 945-963 (1997).
8. R. C. Greenwood et al., *Nature* **435**, 916-918 (2008).
9. D. W. Mittlefehldt et al., In Planetary Materials*Reviews in Mineralogy* **36** (1998).
10. A. W. Beck, H. Y. McSween, *Meteor. Planet. Sci.* **45**, 850-872 (2010).
11. J.-A. Barrat, A. et al. , *Geochim. Cosmochim. Acta* **74**, 6218–6231 (2010).
12. M.C. De Sanctis *et al.*, *Space Sci. Rev.*, DOI 10.1007/s11214-010-9668-5 (2010).
13. C.T. Russell *et al.*, *Science* this issue (2012).
14. A. Coradini et al., *Science* (2011) and reference therein.
15. W.E McClintock, *et al., Science* **321**, 62–65 (2008).
16. J. Veverka *et al.*, *Science* **289**, 2088 (2000).
17. M.T. Capria *et al.*, *Science* this issue (2012).
18. R.G. Burns, *Mineralogical applications of crystal field th*eory, Cambridge Un.Press (1993).
19. P. Schenk *et al., Science* this issue (2012).
20. R. Jaumann *et al, Science* this issue (2012).
21. S. Marchi *et al., Science* this issue (2012).
22. R.N. Clark and T.L. Roush, *J. Geophys Res.* **89**, 6329 (1984).
23. M. J. Gaffey, *J. Geophys Res.* **81,** 905 (1976).
24. L. E. Bowman, M. N. Spilde, J. J. Papike, *Meteoritics Planet. Sci.* **32,** 869-875 (1997).
25. J. S. Delaney, M. Prinz, H. Takeda Proceedings, 15th Lunar and Planetary Science Conference, Part 1, *J. Geophys. Res.*, Supplement **89,** C251-C288 (1984).
26. H. J. Melosh, *Impact Cratering a Geologic Process,* Oxford Univ. Press, Oxford (1989).

SOM

VIR Survey Data

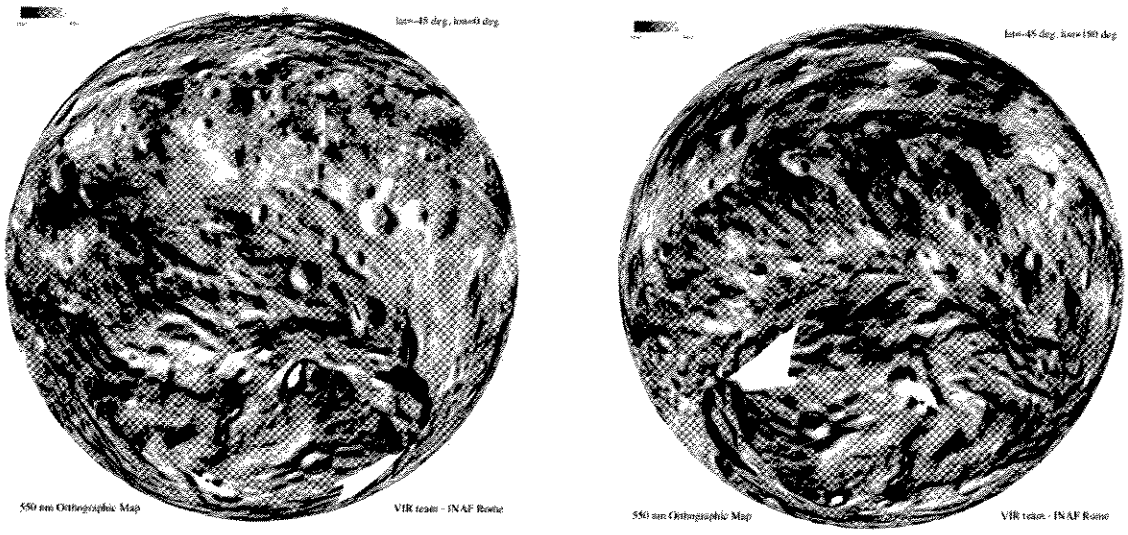

Fig. 1. The two panels show orthographic projections of the 550 nm VIR band. Left: map centered at Lat= -45°, Long=0°; right: map centered at Lat= -45°, Long=180° . The maps were made by combining data that were filtered for angles of incidence and emission <85°. Lommell-Seelinger photometric correction has been applied to the data. The green dots locate the position of the south pole.

Band Parameters

The band centers were computed with the following steps:

1. Smoothing of the spectra (fig 2a).The spectra have been smoothed with a boxcar average of 3 spectral channels.
2. Evaluation of the continuum and continuum removal. The BI continuum has been computed as the straight line between 0.7 and 1.2 micron; the BII continuum has been computed as the straight line between 1.45 and 2.5 micron.
3. Band centers: after the continuum removal, a polynomial fit around the band minima has been computed. Band center is the wavelength which corresponds to the minimum of the second order polynomial fit (fig2b) around the minima of spectra.

Band depths are defined as 1-Rc/Rb, where Rb is the reflectance at the band minimum and Rc is the reflectance of the continuum at the same wavelength as Rb.

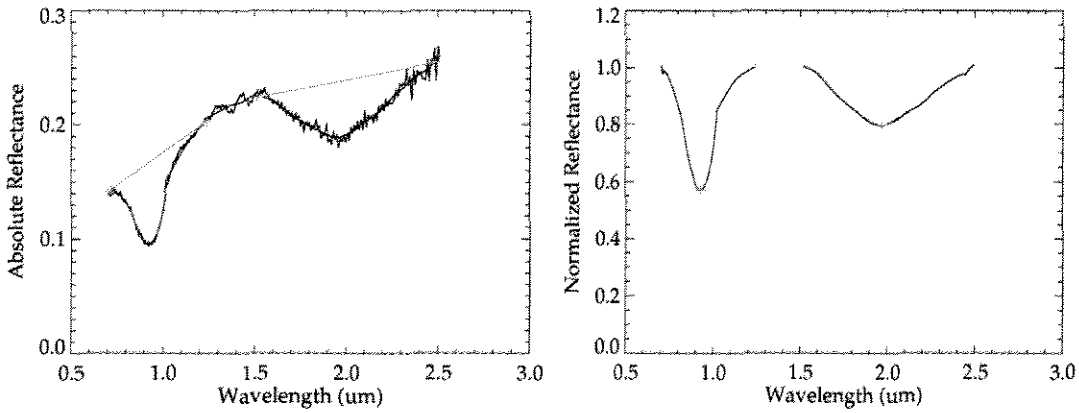

Fig.2. Right: example of Vesta spectrum (black line) with superimposed the smoothed spectrum (red line). The yellow lines represents the straight line used to compute the continuum. Left: continuum removed spectrum (black line) with superimposed the polynomial fit (red line). The yellow cross indicate the BI and BII center.

Bright and Dark areas

From the data, many bright and dark areas are evident. The bright areas show distinct spectral behavior with respect to the surrounding areas, with larger reflectance in the VIS range (550 nm) and deeper bands. Some very bright areas have a visible continuum much brighter (40%) than surrounding areas. Using data from the IR channel we can see that bright regions correspond to regions with low thermal emission (low temperature). Moreover, these areas are usually characterized by deeper pyroxene bands (fig.3).

The dark deposits seen by VIR have lower visual reflectance and higher thermal emission. This behavior provides confirmation that the dark appearance in the VIS range reflects albedo and not shadows. Shadowed areas, in fact, appear cold at 5 μm like the interior walls of some craters. These low-albedo regions have shallower 1 and 2 μm bands (fig 3). For extremely dark areas, the signatures of pyroxenes, especially the 2 μm bands, are strongly reduced with respect to nearby terrains.

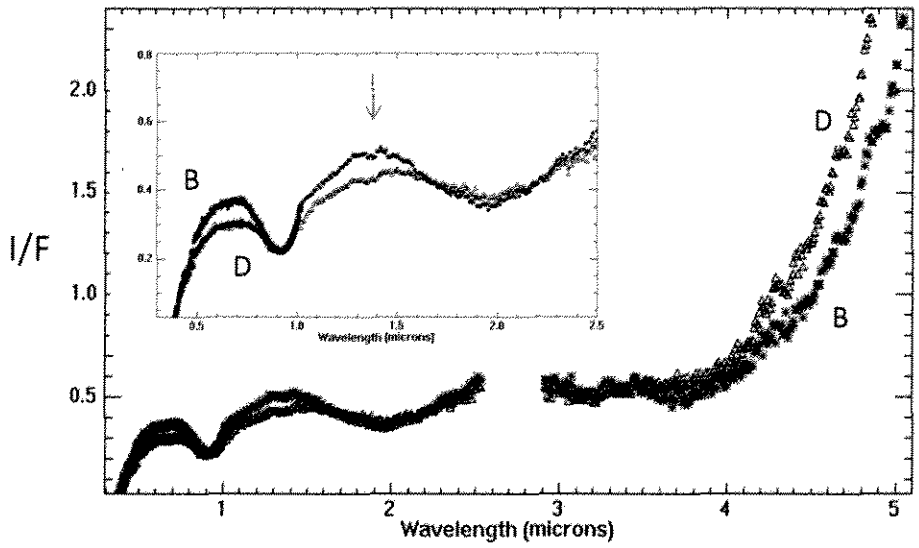

Fig. 3. Spectra of two small areas on Vesta surface: D corresponds to a dark area and B to a bright area. The bright area (B) shows deeper band depths with respect to the dark area (D). The visually dark material (D) shows higher thermal emission than does the visually bright material (B). Artifacts are present in the spectra at ~1.4 μm (arrow).

Vesta and HED spectral comparison

Vesta spectra, on average, resemble those of howardites. Howardites are polymict breccias, consisting of fragments embedded in a matrix of material. The clasts are mostly eucritic and diogenitic in nature, although mixed in with these are rocks of a different origin (most notably dark clasts that have the composition of carbonaceous chondrites, together with impact melt clasts). Howardites should be considered as samples of the asteroid's regolith, which were subsequently altered and ejected, possibly during the impact that created the Vesta's south polar basin.

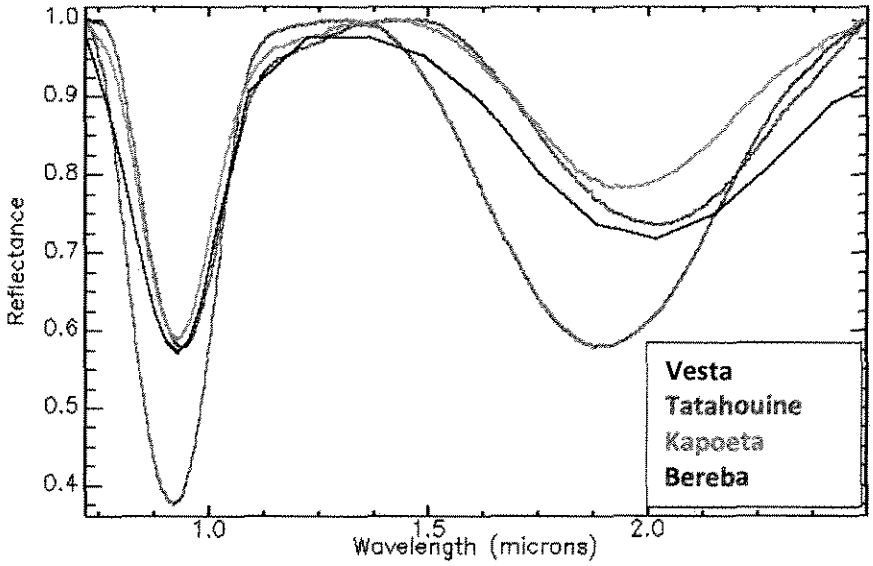

Fig.4: Comparison between a typical Vesta spectrum obtained by VIR and HED spectra (from Relab). VIR spectrum has been smoothed with a boxcar of 9 points.